Z. Phys. Chem. **219** (2005) 197–211

The Rates of the Elementary Reactions of $NH(a^1\Delta)$ with $NH_3(\tilde{X})$ and $HN_3(\tilde{X})$. The Temperature Dependences

By L. Adam[1], W. Hack[1,*], and M. Olzmann[2]

[1] Max-Planck-Institut für biophysikalische Chemie, Am Fassberg 11, 37077 Göttingen, Germany
[2] Institut für Physikalische Chemie, Universität Karlsruhe, Kaiserstr. 12, 76128 Karlsruhe, Germany

(Received September 9, 2004; accepted in revised form November 8, 2004)

Kinetics / Laser-Photolysis / Laser-Induced Fluorescence / Complex-Forming Bimolecular Reaction

The reactions $NH(a) + HN_3(\tilde{X}) \rightarrow$ prod. (1)
and $NH(a) + NH_3(\tilde{X}) \rightarrow$ prod. (2)

were studied in a quasi-static reaction cell in the temperature range $293 \leq T/K \leq 501$ at a pressure of 10 mbar and 20 mbar, respectively, with He as the main carrier gas. The electronically excited reactant NH(a) was generated by laser-flash photolysis of HN_3, at $\lambda = 308$ nm and detected by laser-induced fluorescence (LIF). Also the ground state species NH(X) was detected by LIF.

From the measured concentration-time profiles of NH(a) under pseudo-first order conditions, the rate coefficients $k_1(T)$ and $k_2(T)$ were obtained.

For the rate coefficient k_1 a positive temperature dependence was observed:

$$k_1(T) = (8.1 \pm 0.5) \times 10^{13} \exp[(-0.76 \pm 0.05)/RT]\,\mathrm{cm^3/mol\,s}$$

with a small activation energy of $E_A = 0.76$ kJ/mol.

For reaction (2) the rate coefficient

$$k_2(T) = (8.6 \pm 0.6) \times 10^{13}\,(T/298)^{-(0.6\pm0.1)}\,\mathrm{cm^3/mol\,s}$$

with a negative temperature dependence was measured indicating that the intermediate N_2H_4, which decomposes to $2\,NH_2$, is formed without a barrier.

* Corresponding author. E-mail: whack@gwdg.de

The rate of the quenching channel

$$NH(a) + NH_3 \rightarrow NH(X) + NH_3 \qquad (2q)$$

has the same temperature dependence as the rate of the overall reaction (2). The contribution $k_{2q}/k_2 = 0.008$ over the temperature range $293 \leq T/\mathrm{K} \leq 501$.

1. Introduction

The gaseous detonation of hydrazoic acid HN_3 and the decomposition mechanism of HN_3 have been studied experimentally for many years [1–3]. For the detonation propagation models the knowledge of the chemical kinetics is of vital importance. One of the key reaction in HN_3 decomposition mechanism is the reaction of $NH(a^1\Delta)$ with HN_3 [3]. The rate coefficient and in particular its temperature dependence is thus essential for the understanding of the detonation structure. Moreover, HN_3 is often used as a precursor for the photochemical production of NH(a) and NH(X). Also in the description of these systems the rate coefficient of the reaction

$$NH(a) + HN_3 \rightarrow \text{prod.} \qquad (1)$$

should be known. Reaction (1) has been intensively studied both experimentally [4, 5] and theoretically [6] and is assumed to essentially produce vibronically excited $NH_2(\tilde{A}^2A_1)$ [7, 8], the chemiluminescence of which was used to study the kinetics [5, 9, 10]. To our knowledge the temperature dependence of the rate coefficient, however, has not yet been determined experimentally. In a laser-photolysis experiment of HN_3 at low pressure [5], by detecting the visible emission of $NH_2(\tilde{A}^2A_1)$, the rate coefficient of reaction (1) was observed to depend on the photolysis wavelength. The rate was found to be lower at $\lambda_{ph} = 193$ nm than at $\lambda_{ph} = 266$ nm. An *ab initio* MO investigation on the reactivity of the NH(a) radical in the bimolecular abstraction gas-phase reaction with the HN_3 molecule predicts a barrier height of 12.1 kJ/mol [6].

The reaction of NH with NH_3 is of importance in ammonia and hydrazine pyrolysis and also in the combustion kinetics of N-containing fuels. The reaction of NH(X), *i.e.*, NH in the electronic ground state, has a high activation energy of $E_A = 112$ kJ/mol [2], whereas the reaction of the electronically excited $NH(a^1\Delta)$,

$$NH(a^1\Delta) + NH_3(\tilde{X}) \rightarrow \text{prod.} \qquad (2)$$

has a rate coefficient near the collision limit already at room temperature. The rate coefficient for the reaction of the next higher singlet state, $NH(b^1\Sigma^+)$, however, is again two orders of magnitude smaller than k_2 at room temperature. Its temperature dependence is complicated probably due to the competition between a direct and a complex-forming mechanism [11].

Reaction (2) is assumed to proceed via highly vibrationally excited N_2H_4 in the electronic ground state [12, 13]. The rate coefficient was determined at room temperature [14–16], but its temperature dependence has not yet been investigated. We note that the isoelectronic radical $CH_2(\tilde{a})$ reacts with NH_3 in an insertion reaction with a rate coefficient $k = 1.7 \times 10^{14}$ $(T/295\,\mathrm{K})^{-1.2}\,\mathrm{cm^3/mol\,s}$ in the temperature range $210 \leq T/\mathrm{K} \leq 475$ [17, 18].

2. Experimental

The experiments were performed in a quasistatic laser-flash photolysis/laser-induced fluorescence (LIF) system, where "quasistatic" means that the flow through the reaction cell is negligible between the pump and the probe pulse but sufficient to exchange the gas volume between two subsequent pump pulses. The carrier gas was He at a total pressure of 10 mbar and 20 mbar, respectively.

The temperature was varied in the cell via a copper inset with four perpendicular openings for the laser beams and the observation of the laser-induced fluorescence. The temperature was varied in the range $293 \leq T/\mathrm{K} \leq 501$ and measured by a resistance thermometer with an accuracy ± 0.1 K.

The experimental set up is described in detail elsewhere [19], and only the essentials are repeated here. For the photolysis, a XeCl-exciplex laser (Lambda Physik LPX 205) with pulse energies in the range $200 \leq E/\mathrm{mJ} \leq 400$ and a beam area of about $1.1\,\mathrm{cm^2}$ was used. The probe laser was a dye laser (Lambda Physik FL 3002) with a beam area of $7\,\mathrm{mm^2}$. It was pumped by an exciplex laser (Lambda Physik LPX205, XeCl; $230 \leq E/\mathrm{mJ} \leq 290$).

The NH(a) radicals were produced by HN_3 photolysis in the $\tilde{A} - \tilde{X}$ band at $\lambda = 308$ nm with a rotational excitation significantly above room temperature. The rotationally hot population, however, relaxes to a thermal distribution mainly by collisions with He on a μs time scale.

NH(a, $v = 0$) was detected by exciting the P_3 line at $\lambda = 326.22$ nm of the transition $c^1\Pi$, $v' = 0 \leftarrow a^1\Delta$, $v'' = 0$. The undispersed fluorescence from the excited state was observed in the wavelength range $325 \leq \lambda/\mathrm{nm} \leq 328$ perpendicular to the laser beam using filters (long pass filter KV370 (Schott) or interference filter 326.3 nm (Schott)) to suppress scattered radiation from the excitation beam.

Gases with the highest commercially available purity were used: He, 99.9999%, Praxair; NH_3, 99.998%, UCAR; and N_2, 99.995%, UCAR. HN_3 was synthesized by melting stearic acid, $CH_3(CH_2)_{16}$ COOH, with NaN_3. It was dried with $CaCl_2$ and stored in a bulb at partial pressures ≤ 200 mbar diluted with He (overall pressure ca. 1 bar). For safety reasons, the HN_3 containing devices were covered with a wooden box since HN_3 is highly explosive even at low pressures.

3. Results and discussion

The reactions (1) and (2) were studied under pseudo-first order conditions with the precursor hydrazoic acid and ammonia in large excess over the imino radicals. In this system the NH(a) radicals also react with the precursor molecules,

$$\mathrm{NH(a)} + \mathrm{HN_3} \rightarrow \text{products} \tag{1}$$

and, hence, the depletion of NH(a) has to be described by:

$$-\mathrm{d[NH(a)]}/\mathrm{d}t = k_1[\mathrm{NH(a)}][\mathrm{HN_3}] + k_2[\mathrm{NH(a)}][\mathrm{NH_3}] + k_q[\mathrm{NH(a)}][\mathrm{He}]\,. \tag{I}$$

Since all terms in Eq. (I) are first-order with respect to the imino radical, they can be combined to give:

$$-\mathrm{d[NH(a)]}/\mathrm{d}t = k_{\mathrm{eff}}[\mathrm{NH(a)}]\,. \tag{I′}$$

In general, the physical quenching of NH(a) by He can be neglected, because the rate $k_q < 6 \times 10^8\ \mathrm{cm^3\,mol^{-1}\,s^{-1}}$ [21] is too small. To determine the rate of the NH(a) + $\mathrm{HN_3}$ reaction, experiments without $\mathrm{NH_3}$ were performed and Eq. (I) reduces to:

$$-\mathrm{d[NH(a)]}/\mathrm{d}t = k_1[\mathrm{NH(a)}][\mathrm{HN_3}] = k_{\mathrm{eff}}[\mathrm{NH(a)}]\,. \tag{II}$$

The rate coefficient k_{eff} is determined from plots of $\ln(I(t)/I_{\mathrm{o}})$ *versus* reaction time, where $I(t)$ is the fluorescence intensity due to NH(a) at a given time t, and I_{o} the fluorescence intensity at $t = 0$. The experimental details are summarized in Table 1. The $\mathrm{HN_3}$ concentration was varied in the range $1.2 \leq [\mathrm{HN_3}]/10^{-10}\ \mathrm{mol/cm^3} \leq 10$. In all cases straight lines k_{eff} *vs.* $[\mathrm{HN_3}]$ were obtained, and from the slopes of these lines k_1 was determined; the results are also contained in Table 1. The room temperature rate coefficient of reaction (1) has been previously determined by several groups [8, 9, 19–22, 28]. The values vary in the range from 5.6×10^{13} up to $11 \times 10^{13}\ \mathrm{cm^3/mol\,s}$. The value we obtained, $k_1(293\ \mathrm{K}) = (5.9 \pm 0.5) \times 10^{13}\ \mathrm{cm^3/mol\,s}$, is in good agreement with the results given in some of the more recent publications. In the present work, however, we emphasize the temperature dependence of k_1. The rate coefficient slightly increases with increasing temperature, and from the plot shown in Fig. 1, the following Arrhenius equation is obtained:

$$k_1(T) = (8.1 \pm 0.5) \times 10^{13} \exp[(-0.76 \pm 0.05)\mathrm{kJ\,mol^{-1}/RT}]\ \mathrm{cm^3/mol\,s}\,.$$

This is the first direct determination of the temperature dependence of the rate coefficient k_1.

In a laser photolysis experiment by Watanabe *et al.* [5], $\mathrm{HN_3}$ was decomposed at very low pressures ($p = 40\ \mu\mathrm{bar}$ with no buffer gas) and two different

Table 1. Experimental results for reaction (1): NH(a) + HN_3 → products.

T [K]	p [mbar]	[HN_3] [10^{-10} mol/cm^3]	t-range [μs]	k_{eff} [10^4 s^{-1}]	k_1 [10^{13} cm^3/mol s]
293	20.1	2.1	0–230	1.49	
293	20.1	2.9	0–230	1.86	
293	20.0	4.0	0–140	2.75	
293	20.0	5.5	0–120	2.97	
293	20.1	10.0	0–60	5.77	(5.9 ± 0.5)
360	20.0	1.7	0–230	1.22	
360	20.0	2.4	0–230	1.62	
360	20.0	3.3	0–140	1.96	
360	20.1	4.5	0–120	2.68	
360	20.1	8.1	0–70	5.21	(6.3 ± 0.5)
414	19.9	1.5	0–230	0.98	
414	20.0	2.1	0–230	1.42	
414	20.1	2.8	0–140	2.02	
414	20.0	3.9	0–120	2.26	
414	20.0	7.1	0–70	4.69	(6.5 ± 0.5)
460	20.0	1.3	0–230	0.85	
460	20.0	1.8	0–230	1.33	
460	20.1	2.5	0–140	1.73	
460	20.1	3.5	0–120	2.06	
460	20.1	6.4	0–70	4.16	(6.5 ± 0.5)
501	20.1	1.2	0–230	0.71	
501	20.0	1.7	0–230	1.16	
501	20.1	2.3	0–140	1.85	
501	20.0	3.2	0–120	1.99	
501	20.1	5.9	0–70	3.98	(6.8 ± 0.5)

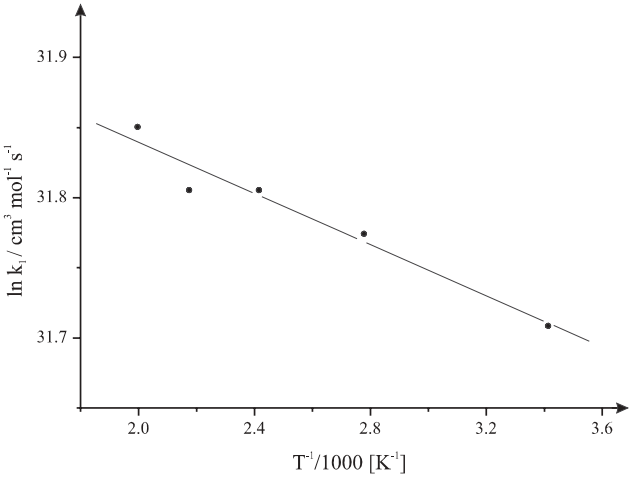

Fig. 1. Temperature dependence of k_1 in an Arrhenius plot.

wavelengths, $\lambda = 266$ nm and $\lambda = 193$ nm. Reaction (1) was observed by time-resolved measurement of the emission of $NH_2(\tilde{A}^2A_1,0,\nu_2',0\text{-}\tilde{X}^2B_1,0,0,0)$, where a lower rate of reaction was observed at $\lambda = 193$ nm than at $\lambda = 266$ nm. Since the NH(a) radicals formed in the photolysis did only undergo collision with HN_3, it was concluded that the higher collisional energy leads to a lower reaction probability. A decrease of the rate coefficient with increasing translational energy indicates a negative temperature dependence. This, however, is not observed in our direct thermal experiment. Henon and Bohr [6] calculated barrier heights for the direct H-abstraction channel of reaction (1) on different CASSCF levels. The authors considered the result obtained from an MRCI approach as most reliable, which yields a classical barrier height of 12.1 kJ/mol. Combined with molecular data from UHF/SSANO computations and by including a simple Wigner correction for tunneling, a rate coefficient of 3.7×10^{12} cm^3/mol s at $T = 300$ K and a thermal activation energy of 0.4 kJ/mol in the temperature range 300–500 K is obtained [6]. Whereas the activation energy is in reasonable agreement with our experimental result, the absolute value of the rate coefficient is underestimated by more than an order of magnitude. This can be due to the fact that the overall reaction may consist of more than just the H-abstraction channel. It is well known that different reaction products can be generated in highly exothermic bimolecular reactions due to the anisotropy of the interaction potential [23–26]. Often abstraction and association channels compete, and a reasonable theoretical description of the overall reaction requires a detailed treatment of the reaction dynamics, for instance, by classical trajectory calculations, on a multi-dimensional potential energy surface. In the present case, besides H abstraction, also addition and insertion reactions are conceivable, and insofar the agreement noted between the experimental and calculated activation energy could be coincidental.

In order to obtain more information about the mechanism of reaction (1), it is useful to compare the temperature dependence of the rate coefficient with that for other elementary reactions of NH(a). For the saturated hydrocarbons CH_4 and C_3H_8 activation energies $E_A = 7.8$ kJ/mol and $E_A = 3.42$ kJ/mol, respectively, were observed [22]. In these cases, insertion into the C–H bond was concluded to be the main mechanism [27]. For the unsaturated hydrocarbons C_2H_4, cis-2-butene, and methyl acetylene, however, no or a negative temperature dependence of the rate coefficients was observed, which was interpreted with an addition mechanism [22]. If we follow this argumentation, the small but positive temperature dependence of the rate coefficient k_1 leads to the interpretation that reaction (1) is likely to proceed via an insertion mechanism, whereas reaction (2) with a slightly negative temperature dependence of k_2 probably proceeds via an addition step (see below).

The NH(a) + NH_3 reaction was studied by adding a large excess of ammonia. For the determination of $k_2(T)$ much lower HN_3 concentrations than in the above given experiments were applied. The relevant conditions are collected in

Table 2. Experimental results for reaction (2): NH(a) + NH_3 → products.

T [K]	p [mbar]	$[HN_3]$ [10^{-11} mol/cm^3]	$[NH_3]$ [10^{-9} mol/cm^3]	t-range [μs]	k_{eff} [10^5 s^{-1}]	$\langle k_{eff} - k_1[HN_3]\rangle$ [10^5 s^{-1}]	k_2 [10^{13} cm^3/mol s]
293	10.1	6.3	0	0–250	0.04		
293	10.0	6.3	1.0	0–50	0.84		
293	10.0	6.3	1.0	0–50	0.85		
293	10.0	6.3	1.0	0–50	0.85	0.81	
293	10.1	6.3	1.8	0–28	1.58		
293	10.1	6.3	1.8	0–27	1.58		
293	10.0	6.3	1.8	0–27	1.57	1.54	
293	9.9	6.3	2.7	0–17	2.25		
293	10.0	6.3	2.7	0–16	2.34		
293	9.9	6.3	2.7	0–17	2.35	2.27	
293	10.0	6.3	3.9	0–11	3.59		
293	10.1	6.3	3.9	0–11	3.36		
293	10.0	6.3	3.9	0–11	3.55	3.46	(8.7 ± 0.7)
360	10.0	5.1	0	0–250	0.04		
360	10.0	5.1	0.8	0–50	0.61		
360	10.1	5.1	0.8	0–50	0.61	0.57	
360	10.0	5.1	1.5	0–26	1.22		
360	10.0	5.1	1.5	0–26	1.09	1.12	
360	9.9	5.1	2.2	0–17	1.63		
360	10.1	5.1	2.2	0–17	1.64	1.60	
360	10.1	5.1	3.2	0–11	2.50		
360	10.0	5.1	3.2	0–11	2.43	2.43	(7.5 ± 0.6)

Table 2. Reaction (2) was studied at a pressure of 10 mbar under pseudo first-order conditions in the concentration ratio range $(0.95 \preceq [NH_3]_0/[NH(a)]_0 \preceq 6.2) \times 10^4$, and the results are given in Table 2. The depletion of NH(a) solely by the precursor molecule HN_3 was measured in independent experiments ($[NH_3]_0 = 0$, see above). At room temperature, they lead to a pseudo-first order rate coefficient $k_1[HN_3] = 4.0 \times 10^3\,s^{-1}$, which corresponds to

Table 2. continued.

T [K]	p [mbar]	[HN_3] [10^{-11} mol/cm^3]	[NH_3] [10^{-9} mol/cm^3]	t-range [μs]	k_{eff} [10^5 s^{-1}]	$\langle k_{eff} - k_1[HN_3] \rangle$ [10^5 s^{-1}]	k_2 [10^{13} cm^3/mol s]
414	9.9	4.5	0	0–250	0.04		
414	10.0	4.5	0.7	0–60	0.52		
414	9.9	4.5	0.7	0–60	0.54	0.49	
414	10.1	4.5	1.3	0–28	1.03		
414	10.1	4.5	1.3	0–28	0.97	0.96	
414	10.0	4.5	1.9	0–18	1.26		
414	9.9	4.5	1.9	0–18	1.36	1.27	
414	10.0	4.5	2.8	0–12	1.82		
414	10.0	4.5	2.8	0–12	1.97	1.86	(6.8 ± 0.5)
460	10.0	4.0	0	0–250	0.05		
460	10.0	4.0	0.6	0–50	0.46		
460	10.0	4.0	0.6	0–50	0.44	0.40	
460	10.1	4.0	1.1	0–30	0.78		
460	10.0	4.0	1.1	0–30	0.81	0.75	
460	10.1	4.0	1.7	0–20	1.11		
460	10.1	4.0	1.7	0–20	1.18	1.10	
460	10.0	4.0	2.5	0–15	1.68		
460	10.0	4.0	2.5	0–15	1.66	1.62	(6.5 ± 0.5)

$k_1 = 6.3 \times 10^{13}$ cm^3/mol s in good agreement with the above given results and the value of $k_1 = 7.2 \times 10^{13}$ cm^3/mol s reported in Ref. [28]. The contribution of reaction (1) to the depletion was measured independently for all experimental conditions. These correction terms (listed in Table 2 for $[NH_3] = 0$) are subtracted from k_{eff} (as determined by Eq. (I′)) and lead to the first order rate coefficients which are listed in Table 2. The average is taken for each set of am-

Table 2. continued.

T [K]	p [mbar]	$[HN_3]$ [10^{-11} mol/cm^3]	$[NH_3]$ [10^{-9} mol/cm^3]	t-range [μs]	k_{eff} [10^5 s^{-1}]	$\langle k_{eff} - k_1[HN_3]\rangle$ [10^5 s^{-1}]	k_2 [10^{13} cm^3/mol s]
501	9.9	3.7	0	0–250	0.05		
501	10.0	3.7	0.6	0–60	0.39		
501	10.1	3.7	0.6	0–60	0.40		
501	10.0	3.7	0.6	0–60	0.42	0.35	
501	10.1	3.7	1.1	0–30	0.71		
501	10.0	3.7	1.1	0–30	0.73		
501	10.0	3.7	1.1	0–30	0.69	0.66	
501	9.9	3.7	1.6	0–20	1.05		
501	10.0	3.7	1.6	0–20	1.06		
501	10.1	3.7	1.6	0–20	0.96	0.97	
501	10.1	3.7	2.3	0–15	1.51		
501	10.0	3.7	2.3	0–15	1.50		
501	10.0	3.7	2.3	0–15	1.67	1.51	(6.3 ± 0.5)

monia concentrations. We note that the depletion of NH(a) by HN_3 is slightly faster at higher temperatures in agreement with the above experiments. The values of k_2 in Table 2 are obtained from the slope of the plots of the averaged first-order rate coefficients *vs.* $[NH_3]$. Two of these plots, for the lowest and highest temperature, are shown in Fig. 2. For all temperatures straight lines through the origin were obtained. For room temperature the slope provides the

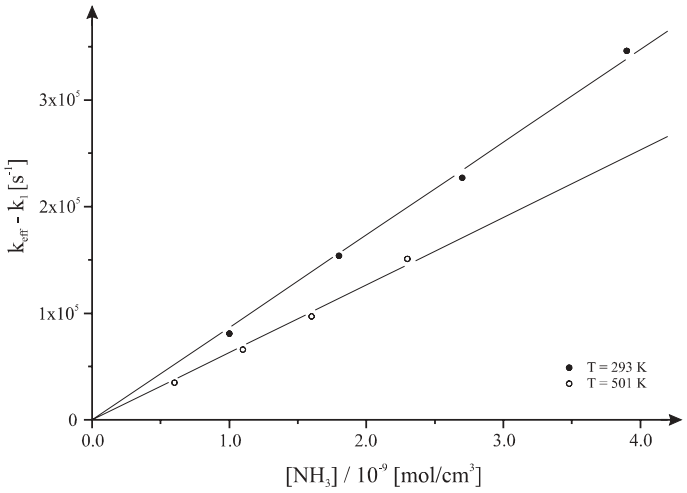

Fig. 2. First order rate coefficient for reaction (2) *versus* $[NH_3]$ for the highest and lowest temperature studied.

second-order rate coefficient:

$$k_2(293\,\mathrm{K}) = (8.7 \pm 0.7) \times 10^{13}\,\mathrm{cm^3/mol\,s},$$

which is in good agreement with the values $k_2 = 8.8 \times 10^{13}\,\mathrm{cm^3/mol\,s}$ and $k_2(9.1 \pm 0.9) \times 10^{13}\,\mathrm{cm^3/mol\,s}$ determined earlier in our laboratory [15, 16]. For $T = 501\,\mathrm{K}$ a rate coefficient of $k_2(501\,\mathrm{K}) = (6.3 \pm 0.5) \times 10^{13}\,\mathrm{cm^3/mol\,s}$ is obtained from the plot in Fig. 2; this is smaller than the value at room temperature.

The rate coefficients k_2 were measured in the temperature range $293 \leq T/\mathrm{K} \leq 501$, and the results are collected in Table 2. They show a decrease with increasing temperature, and a plot of $\ln k_2$ *versus* $\ln T$ is displayed in Fig. 3. From the plot a temperature dependence of the form

$$k_2(T) = (8.6 \pm 0.6) \times 10^{13} (T/298\,\mathrm{K})^{-0.6\pm0.1}\,\mathrm{cm^3/mol\,s}$$

can be derived. This is the first measurement of the temperature dependence of this rate coefficient.

The main pathway of reaction (2) under these experimental conditions is the decomposition of the electronic chemically activated hydrazine into two NH_2 radicals:

$$\mathrm{NH(a) + NH_3(\tilde{X}) \rightarrow N_2H_4(\tilde{X}^*) \rightarrow 2NH_2}\,.$$

The quenching channel:

$$\mathrm{NH(a) + NH_3(\tilde{X}) \rightarrow NH(X) + NH_3} \qquad \text{(2q)}$$

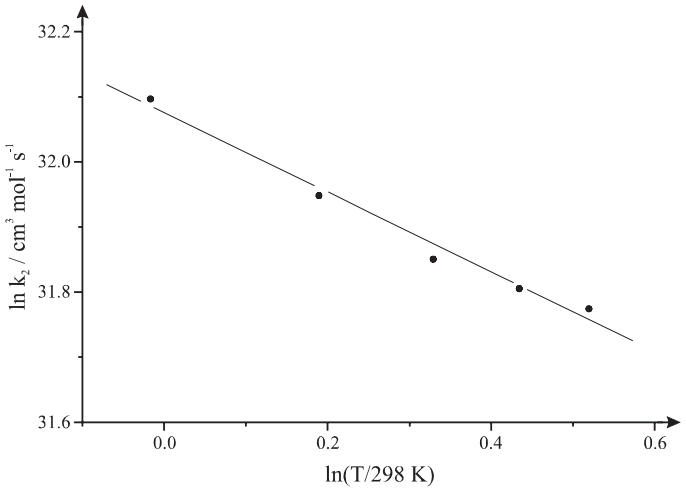

Fig. 3. Temperature dependence of the second order rate coefficient k_2 in the temperature range $293 \leq T/K \leq 501$.

was found to be unimportant at room temperature [15]. In the present study, we also measured the contribution of the quenching in the temperature range given above, relating the NH(X) formation via reaction (2q) to the NH(X) formation in the reaction

$$NH(a) + N_2 \rightarrow NH(X) + N_2 \tag{3}$$

under identical experimental conditions. For reaction (3) it is known that NH(X) is the only product. The ratio of NH(X) formation in reactions (2) and (3) is given by $\alpha_{NH(X)} = \frac{[NH(X)]_{(2)}}{[NH(X)]_{(3)}}$ at long reaction times, where $[NH(X)]_{(2)}$ is the NH formed in the quenching channel of reaction (2) and $[NH(X)]_{(3)}$ formed in reaction (3). The experimental results are given in Table 3. There is no significant temperature dependence of the quenching ratio between 293 K and 501 K. The quenching in this temperature range is negligible and the rate coefficient $k_{2q}(T)$ exhibits the same temperature dependence as the overall rate coefficient k_2. Thus, it can be excluded that the small quenching rate coefficient $k_{2q}(298\,\mathrm{K}) = 7 \times 10^{11}\,\mathrm{cm^3/mol\,s}$ at room temperature is caused by a large barrier for the quenching channel.

The very similar temperature dependence of $k_2(T)$ and $k_{2q}(T)$, however, indicates that NH(X) and $NH_2(\tilde{X})$ are likely to be formed via the same mechanism:

$$\begin{aligned} NH(a) + NH_3(\tilde{X}) \rightarrow N_2H_4(\tilde{X}^*) &\rightarrow 2NH_2(\tilde{X}) \\ &\rightarrow NH(X) + NH_3 \end{aligned}$$

Table 3. Experimental results for the quenching ratio $\alpha_{[NH(X)]}$ in reaction (2).

T [K]	p [mbar]	$[HN_3]$ $[10^{-11}$ mol/cm$^3]$	$[NH_3]$ $[10^{-9}$ mol/cm$^3]$	$[N_2]$ $[10^{-7}$ mol/cm$^3]$	Δt [μs]	$I^{NH_3}_{NH(X)}$ $[10^{-3}$ a.u.]	$I^{N_2}_{NH(X)}$ $[10^{-1}$ a.u.]	$\alpha_{NH(X)}$ [%]
293	20.1	4.0	2.0	0	140	2.08	–	
293	20.0	4.0	2.0	0	140	2.00	–	(0.8 ± 0.2)
293	20.0	4.0	0	8.2	140	–	2.42	
293	20.1	4.0	0	8.2	140	–	2.45	
360	20.0	3.3	2.0	0	140	1.52	–	
360	20.0	3.3	2.0	0	140	1.62	–	(0.8 ± 0.2)
360	19.9	3.3	0	6.7	140	–	1.88	
360	20.1	3.3	0	6.7	140	–	1.94	
414	20.0	2.8	2.0	0	140	1.20	–	
414	20.1	2.8	2.0	0	140	0.98	–	(0.7 ± 0.2)
414	20.0	2.8	0	5.8	140	–	1.43	
414	20.0	2.8	0	5.8	140	–	1.41	
460	20.0	2.5	2.0	0	140	1.15	–	
460	20.0	2.5	2.0	0	140	1.37	–	(0.7 ± 0.2)
460	20.1	2.5	0	5.2	140	–	1.84	
460	20.1	2.5	0	5.2	140	–	1.82	
501	20.0	2.3	2.0	0	140	1.65	–	
501	20.0	2.3	2.0	0	140	1.60	–	(0.7 ± 0.2)
501	20.0	2.3	0	4.8	140	–	2.20	
501	20.0	2.3	0	4.8	140	–	2.21	

i.e., vibrationally excited hydrazine in the electronic ground state $N_2H_4(\tilde{X}^1A^*)$ decomposes to a small portion (< 1%) into NH(X) and ammonia.

In the following, we discuss the temperature dependence of k_2 with respect to possible reaction mechanisms.

As already mentioned above, the reactions of NH(a) with saturated hydrocarbons have rate coefficients with weakly positive temperature dependence [22] and probably proceed via a direct insertion of NH(a) into a σ bond [27, 29]. Reactions of NH(a) with unsaturated hydrocarbons, however, exhibit no or slightly negative temperature dependences [22], and quantum chemical calculations indicate that these reactions are likely to start with a cycloaddition of NH(a) to the π bond of the hydrocarbon [30]. The reactions of NH(a) with compounds bearing lone electron pairs seem to resemble these reactions with unsaturated species. Sudhakar and Lammertsma [31] have shown by ab initio calculations that the reactions of NH(a) with H_2O, H_2S, and HCl at first lead to donor-acceptor complexes, and that subsequent hydrogen migrations yield the more stable tautomers. This model can be used to interpret experimental results of Okada *et al.* on the reactions NH(a) + CH_3OH and NH(a) + CH_3OD [32]. Whereas the rate coefficients for both isotopomers do not significantly differ, the product branching ratio [NHD]/[NH_2] for the NH(a) + CH_3OD reaction is (23 ± 9). These findings can be explained by assuming that the rate coefficients are determined by the barrier-less association reactions NH(a) + $CH_3OH \rightarrow CH_3O(NH)H$ and NH(a) + $CH_3OD \rightarrow CH_3O(NH)D$, respectively, whereas the branching ratio is governed by the different rates of the two conceivable tautomerizations with subsequent fast C–N bond dissociation. Obviously, the 1,2 hydrogen shift from the O to the N atom is much faster than the 1,3 hydrogen shift from the C to the N atom. Hence, there is no isotope effect in the rate coefficients but a considerable deuterium enrichment in the amino radical from the NH(a) + CH_3OD reaction. From other barrier-less association reactions like radical-radical or ion-molecule capture, it is well known that their rate coefficients often have no or slightly negative temperature dependences [33, 34].

In line with these arguments, we rationalize the absolute magnitude as well as the negative temperature dependence of k_2 using an association-isomerization mechanism originally proposed by Pople *et al.* ([12], see also [13, 35]). These authors concluded from ab initio calculations that NH(a) and $NH_3(\tilde{X})$ at first form an energized adduct HN–NH_3*, which subsequently isomerizes to give electronic chemically activated hydrazine H_2N–$NH_2(\tilde{X}^1A)$* that finally decomposes to produce two NH_2 radicals [15, 16]. The isomerization barrier is much lower than the energy of back-dissociation, and in Ref. [16] we estimated that under low-pressure conditions only 0.3% of the energized HN–NH_3* adduct dissociate back to NH(a) + NH_3, whereas 99.7% isomerize and finally decompose to NH_2 + NH_2. Hence, the overall rate coefficient k_2 is capture-controlled and independent of pressure under our experimental conditions. In Ref. [16], we performed a simplified SACM calculation [36] and

obtained a value for k_2 at room temperature in reasonable agreement with the experimental result. A reliable prediction of the generally weak temperature dependence of the rate coefficients for such barrierless association reactions, however, is much more difficult. It is well known that, apart from electronic contributions, the details of the intermolecular potential have a large influence (see *e.g.*, [37]). In the model of Ref. [16], we used a Morse function for the interfragment potential and obtained a temperature dependence of $T^{+0.28}$ in contrast to $\sim T^{-0.6}$ in the experiments. Such a slightly positive temperature dependence is often predicted by the simplified SACM based on Morse potentials [38]. Negative temperature dependences can be obtained by using electrostatic potentials, where a dipole-dipole interaction, for instance, would have given $T^{-0.17}$ [37]. Such electrostatic potentials, however, can only be used for very low temperatures, where the main contributions to the centrifugal partition function correspond to the long-range part of the potential [37]. Hence, they are surely not adequate for the temperature range of our experiments. As long as no reliable potential for the NH(a) + NH_3 interaction is available, a more detailed discussion of the temperature dependence would surely be too speculative. Nonetheless, the slightly negative temperature dependence of k_2 indicates that a barrier-less association process is likely to be the initial step of the NH(a) + NH_3 reaction.

Acknowledgement

Thanks are due to the Deutsche Forschungsgemeinschaft (Sonderforschungsbereich 357 “Molekulare Mechanismen unimolekularer Prozesse”) and the Fonds der Chemischen Industrie for financial support.

References

1. O. Kajimoto, T. Yamamoto, and T. Fuerro, J. Phys. Chem. **83** (1979) 429.
2. H. Röhrig and H. Gg. Wagner, Ber. Bunsenges. Phys. Chem. **98** (1994) 1073.
3. C. Paillard, G. Dupré, A. Aitch, and S. Youssefi, Prog. Astronaut. Aeronaut. **133** (1991) 63.
4. W. Hack, in *Gmelin Handbook of Inorganic and Organometallic Chemistry*. Supplement Volume 31 (1993) p. 118 ff. (and references therein).
5. A. Watanabe, K. Yamasaki, and I. Tokue, Laser Chem. **15** (1995) 183.
6. E. Henon and F. Bohr, J. Molec. Struct. THEOCHEM **531** (2000) 283.
7. H. Okabe, J. Chem. Phys. **49** (1968) 2726.
8. J. R. McDonald, R. G. Miller, and A. P. Baronavski, Chem. Phys. Lett. **51** (1977) 57; Chem. Phys. **30** (1978) 133.
9. R. J. Paur and E. J. Bair, Int. J. Chem. Kinet. **8** (1976) 139.
10. K. Yamasaki, A. Watanabe, I. Tokue, and Y. Ito, Chem. Phys. Lett. **204** (1993) 106.
11. A. Höser, M. Blumenstein, F. Stuhl, and M. Olzmann. J. Chem. Soc. Faraday Trans. **93** (1997) 2029.
12. J. A. Pople, K. Raghavachari, M. J. Frisch, J. S. Binkley, and P. V. R. Schleyer, J. Am. Chem. Soc. **105** (1983) 6389.

13. P. V. Sudhakar and K. Lammertsma, J. Am. Chem. Soc. **113** (1991) 1899.
14. R. D. Bower, M. T. Jacoby, and J. A. Blauer, J. Chem. Phys. **86** (1987) 1954.
15. W. Hack and K. Rathmann, Z. Phys. Chem. **176** (1992) 151.
16. L. Adam, W. Hack, and M. Olzmann, Z. Phys. Chem. **218** (2004) 439.
17. R. Wagener, Dissertation, Report 4 MPI für Strömungsforschung Göttingen (1990).
18. M. Koch, F. Temps, R. Wagener, and H. Gg. Wagner, Z. Naturforsch. **44a** (1989) 195.
19. W. Hack and A. Wilms, Z. Phys. Chem. Neue Folge **161** (1989) 107.
20. L. G. Piper, R. H. Krech, and R. L. Taylor, J. Chem. Phys. **73** (1980) 791.
21. F. F. Rohrer and F. Stuhl, Chem. Phys. Lett. **111** (1984) 234.
22. J. W. Cox, H. H. Nelson, and J. R. McDonald, Chem. Phys. **96** (1985) 175.
23. L.B. Harding and A. F. Wagner, Proc. Combust. Inst. **21** (1986) 721.
24. H. Arai, S. Kato, and S. Koda, J. Phys. Chem. **98** (1994) 12.
25. J. P. Simons, J. Chem. Soc., Faraday Trans. **93** (1997) 4095.
26. M. González, J. Hernando, I. Baños, and R. Sayós, J. Chem. Phys. **111** (1999) 8913.
27. W. Hack and K. Rathmann, Ber. Bunsenges. Phys. Chem. **94** (1990) 1304.
28. F. Freitag, F. Rohrer, and F. Stuhl, J. Phys. Chem. **93** (1989) 3170.
29. S. Kodama, J. Phys. Chem. **92** (1988) 5019.
30. T. Fueno, V. Bonačić-Koutecký, and J. Koutecký, J. Am. Chem. Soc. **105** (1983) 5547.
31. P. V. Sudhakar and K. Lammertsma, J. Am. Chem. Soc. **113** (1991) 5219.
32. S. Okada, A. Tezaki, K. Yamasaki, and H. Matsui, J. Chem. Phys. **98** (1993) 8667.
33. I. W. H. Smith, J. Chem. Soc. Faraday Trans. **87** (1991) 2271.
34. J. Troe, in *State-Selected and State-to-State Ion-Molecule Reaction Dynamics Part 2: Theory*, M. Baer, C.-Y. Hy, Eds., Advances in Chemical Physics Series, Vol. LXXXII, Wiley (1992), p. 485.
35. F. Ding and L. Zhang, Int. J. Quantum Chem. **64** (1997) 447.
36. J. Troe, J. Chem. Phys. **75** (1981) 226.
37. J. Troe, Chem. Rev. **103** (2003) 4565.
38. C. J. Cobos and J. Troe, J. Chem. Phys. **83** (1985) 1010.